1838 cm^{-1} for the (TPP)Co(NO)/(TMP)$FeClO_4$ system. The former peak is due to $[(OEP)Fe(NO)]^+$, while the latter is due to $[(TMP)Fe(NO)]^+$.

A positive peak at 1535 cm^{-1} (see Figure 6a) only occurs for the exchange reaction involving (OEP)$FeClO_4$ and $[(TPP)Co(NO)]^+$ and is assigned as the π-cation-radical marker band of $[(OEP)FeClO_4]^+$, which is generated at 1.1 V according to eq 12.[22,45]

$$(OEP)FeClO_4 \overset{E_{1/2} = 1.02\ V}{\rightleftharpoons} [(OEP)FeClO_4]^+ + e^- \quad (12)$$

Conclusion. A nitrosyl ligand transfer can be observed between Fe(II) and Co(II) porphyrins, between Co(II) and Fe(III) porphyrins, and between Fe(III) porphyrins and Co(II) porphyrin cation radicals. The driving force behind these different NO-transfer reactions is related both to the nature of the different central metals of (P)M(NO) and $[(P)M(NO)]^+$ and to the different oxidation states of the complex. The NO transfer is also related to differences in the porphyrin macrocycle although, in the present series of investigated compounds, this effect was not dominant. In summary, the following overall order of stability is observed for the investigated nitrosyl complexes:

$$(P)Fe(NO) > (P)Co(NO) > [(P)Fe(NO)]^+ > [(P)Co(NO)]^+$$

Finally, the data and observations reported in the present paper should prove helpful in understanding the reactions of these biologically important species and should also serve as a basis for comparing other published data on metalloporphyrins containing diatomic molecule adducts.

Acknowledgment. The support of the National Institutes of Health (Grant GM-15172) and the National Science Foundation (Grant CHE-8822881) is gratefully acknowledged.

Registry No. NO, 14452-93-8; (OEP)$FeClO_4$, 50540-30-2; (OEP)Fe(NO), 55917-58-3; (TPP)Co(NO), 42034-08-2; $[(OEP)Fe(NO)]^+$, 89596-92-9; $[(TPP)Co(NO)]^+$, 120544-36-7; (TPP)$FeClO_4$, 57715-43-2; $[(TPP)FeClO_4]^+$, 125138-88-7; $[(TPP)Fe(NO)]^+$, 70622-46-7; (TPP)$CoClO_4$, 76402-67-0; $[(TMP)Fe(NO)]^+$, 117470-06-1; $[(OEP)FeClO_4]^+$, 111436-54-5; (TMP)Fe(NO), 117470-05-0; (TMP)$FeClO_4$, 93862-22-7; $[(TPP)CoClO_4]^+$, 125138-89-8; $[(TMP)FeClO_4]^+$, 125138-90-1; (OEP)Fe, 61085-06-1; (TPP)Co, 14172-90-8; (TPP)Fe(NO), 52674-29-0; CH_2Cl_2, 75-09-2.

(45) Shimomura, E. T.; Phillippi, M. A.; Goff, H. M. *J. Am. Chem. Soc.* **1981**, *103*, 6778.
(46) Truxillo, L. A.; Davis, D. G. *Anal. Chem.* **1975**, *47*, 2260.
(47) Kadish, K. M.; Bottomley, L. A. *Inorg. Chem.* **1980**, *19*, 832.
(48) Swistak, C.; Mu, X. H.; Kadish, K. M. *Inorg. Chem.* **1987**, *26*, 4360.
(49) Kadish, K. M.; Lin, X. Q.; Han, B. C. *Inorg. Chem.* **1987**, *26*, 4161.
(50) Salehi, A.; Oertling, W. A.; Babcock, G. T.; Chang, C. K. *J. Am. Chem. Soc.* **1986**, *108*, 5630.
(51) Fajer, J. Private communication.

Contribution from the Department of Chemistry, University of Houston, Houston, Texas 77204-5641

Synthesis, X-ray Structure, and Characterization of $[(OEP)IrCl]_2$dppe, Where OEP Is the Dianion of Octaethylporphyrin and dppe Is 1,2-Bis(diphenylphosphino)ethane

K. M. Kadish,* Y. J. Deng, and J. D. Korp

Received June 7, 1989

The synthesis and characterization of $[(OEP)IrCl]_2$dppe, where OEP is the dianion of octaethylporphyrin and dppe is 1,2-bis(diphenylphosphino)ethane, are reported. $[(OEP)IrCl]_2$dppe was synthesized from a reaction involving (OEP)$Ir(C_3H_7)$ and dppe in CH_2Cl_2. The bimetallic complex is not generated in benzene solvent, where (OEP)$Ir(C_3H_7)$(dppe) is quantitatively formed instead. Single-crystal X-ray analysis showed $[(OEP)IrCl]_2$dppe to crystallize in the monoclinic space group $P2_1/c$ with cell constants a = 13.989 (4) Å, b = 19.864 (6) Å, c = 17.752 (6) Å, β = 101.22 (2)°, and Z = 2. The Ir atom is out of the porphyrin plane by 0.076 Å toward phosphorus. The compound exhibits a normal UV-visible spectrum in nonaqueous media, as opposed to the hyperspectrum of other Ir(III) porphyrins containing bound phosphine ligands. ^1H NMR data show that all the porphyrin ring protons of $[(OEP)IrCl]_2$dppe are shifted upfield compared to those of monomeric iridium(III) porphyrins, thus suggesting a mutual influence of the ring current. The ethylene group in the bridging dppe ligand is shielded by the two porphyrin moieties, which results in an unusual upfield resonance at −5.74 ppm. $[(OEP)IrCl]_2$dppe undergoes two reversible oxidations and one irreversible reduction in methylene chloride or *n*-butyronitrile at room temperature. The first oxidation involves an overall two-electron-transfer process where one electron is abstracted from each porphyrin ring of the dimer. The product of this reversible oxidation is a biradical, which was characterized by ESR spectroscopy and spectroelectrochemistry. The reduction of $[(OEP)IrCl]_2$dppe in *n*-butyronitrile involes an ECE type mechanism, and the formation of $[(OEP)Ir]^-$ is postulated to occur on the thin-layer spectroelectrochemical time scale after the overall addition of four electrons. However, on the bulk electrolysis time scale, a demetalation of reduced $[(OEP)IrCl]_2$dppe is observed.

Introduction

The electrochemistry of bimetallic porphyrins of the type $[(P)Fe]_2L$ and $[(P)RhCl]_2L$ has been investigated for complexes with both single-atom[1-3] and multiatom[4,5] bridging ligands, L. For some of these porphyrins, there is an interaction across the bridging ligand, while, for others, the two metalloporphyrins are noninteracting. For example, $[(P)Fe]_2L$, where P = the dianion of a given porphyrin and L = C, N, or O, shows significant ligand-mediated metal-metal interactions[1-3] but $[(TPP)Fe]_2L$, when L = pyrazine or 1,2-bis(4-pyridyl)ethylene, shows no interaction between the two iron porphyrin fragments.[5] A recent electrochemical investigation of $[(P)RhCl]_2L$ indicates that the two rhodium porphyrin units can interact when they are connected by a conjugated dibasic nitrogen bridging ligand such as 4,4-bipyridine or *trans*-1,2-bis(4-pyridyl)ethylene.[4] However, when the two Rh(III) complexes are bridged by a nonconjugated dibasic nitrogen bridging ligand such as 1,2-bis(4-pyridyl)ethane or 4,4′-trimethylenebis(pyridine), little if any interaction exists between the two metalloporphyrins.[4] Similar results have been obtained for other non-porphyrin complexes such as $\{[(NH_3)_5Ru]_2L\}^{n+}$ where n = 4, 5, or 6 and L = a 4,4′-dipyridyl type ligand.[6,7]

Bridged bimetallic porphyrins with other central metals or with different types of bridging ligands have not been electrochemically

(1) Lançon, D.; Kadish, K. M. *Inorg. Chem.* **1984**, *23*, 3942.
(2) Kadish, K. M.; Rhodes, R. K.; Bottomley, L. A.; Goff, H. M. *Inorg. Chem.* **1981**, *20*, 3195.
(3) Chang, D.; Cocolios, P.; Wu, Y. T.; Kadish, K. M. *Inorg. Chem.* **1984**, *23*, 1629.
(4) Liu, Y. H.; Anderson, J. E.; Kadish, K. M. *Inorg. Chem.* **1988**, *27*, 2320.
(5) Bottomley, L. A.; Gorce, J.-N. *Inorg. Chem.* **1988**, *27*, 3733.
(6) Creutz, C.; Taube, H. *J. Am. Chem. Soc.* **1969**, *91*, 3988.
(7) (a) Callahan, R. W.; Brown, G. M.; Meyer, T. J. *Inorg. Chem.* **1975**, *14*, 1443. (b) *J. Am. Chem. Soc.* **1974**, *96*, 7829.

0020-1669/90/1329-1036$02.50/0

studied, but the synthesis of numerous transition-metal porphyrin complexes with different bridging ligands is possible.[8,9] Terminal bis(diphenylphosphino)alkanes would seem to be good bridging ligand candidates for metalloporphyrins, since they have excellent binding properties and are known to serve as bridging ligands for various complexes with different transition metals.[10-12]

In a previous study,[13] we reported that phosphorus-containing ligands such as PPh_3 or $P(OEt_3)$ readily bind to iridium(III) porphyrins of the type (OEP)Ir(C_3H_7). The properties of (OEP)Ir(C_3H_7)(PPh_3) and (OEP)Ir(C_3H_7)($P(OEt)_3$) were spectrally and electrochemically characterized in solution, and the former species was also structurally characterized by X-ray methods. The data from this study indicated that the compounds have a strong Ir–P bond and suggested that bimetallic bridged Ir(III) species should be easily generated. This is indeed found to be the case, and we now report the synthesis, X-ray structure, and characterization of [(OEP)IrCl]$_2$dppe, where dppe = 1,2-bis(diphenylphosphino)ethane.

Experimental Section

Instrumentation and Methods. Cyclic voltammetric measurements were obtained with an IBM EC 225 voltammetric analyzer, an EG&G Princeton Applied Research Model 174A/175 polarographic analyzer/universal programmer, or a BAS 100 electrochemical analyzer. A platinum button served as the working electrode, and a platinum wire as the counter electrode. A saturated calomel electrode (SCE), which was separated from the bulk solution by a fritted-glass disk, was used as the reference electrode. Bulk controlled-potential coulometry was performed on an EG&G Princeton Applied Research Model 173 potentiostat which contained a Model 179 coulometer system that was coupled with a Princeton Applied Research Model RE-0074 time base X-Y recorder. Thin-layer spectroelectrochemical measurements were made with an EG&G Princeton Applied Research Model 173 potentiostat coupled with a Tracor Northern 1710 spectrometer/multichannel analyzer or Tracor Northern 6500 rapid-scan spectrometer. Construction of the thin-layer cell is described in the literature.[14] Low-temperature experiments were carried out by cooling the cell to a constant temperature with a dry ice/acetone bath.

UV–visible spectra were recorded on an IBM 9430 spectrophotometer. ^{1}H NMR spectra were recorded on a GE QE-300 spectrometer. An IBM Model 100D electron spin resonance system was used to record ESR spectra.

Materials. HPLC grade methylene chloride (CH_2Cl_2) was distilled from P_2O_5 for electrochemical and spectroelectrochemical experiments, and the same grade CH_2Cl_2 was used for synthetic purposes without further purification. Spectroscopic grade benzene and analytical grade *n*-butyronitrile (PrCN) were used as received. Tetra-*n*-butylammonium perchlorate ((TBA)ClO_4) was purchased from Fluka Chemical Co., purified by two recrystallizations from ethyl alcohol, and stored in a vacuum oven at 40 °C. Unless otherwise noted, 0.1 M (TBA)ClO_4 was used as the supporting electrolyte in the electrochemical and spectroelectrochemical measurements.

1,2-Bis(diphenylphosphino)ethane (dppe) was purchased from Aldrich Chemical Co. and was used without further purification.

Synthesis of [(OEP)IrCl]$_2$dppe. One half equivalent of dppe was slowly added dropwise to a solution of (OEP)Ir(C_3H_7) (20 mg) in CH_2Cl_2 (20 mL) at room temperature. The mixture was stirred for 30 min and the solvent then evaporated under reduced pressure, after which the residue was chromatographed on a silica gel column. The first eluent with benzene was unreacted (OEP)Ir(C_3H_7), which was identified by its UV–visible spectrum (λ_{max} = 388, 500, and 528 nm). The second fraction was eluted with benzene–acetone (1:1) and gave [(OEP)IrCl]$_2$dppe. Recrystallization of this crude product from a benzene–hexane mixture led to 8 mg of the bridged bimetallic iridium(III) porphyrin. Elemental analysis was performed by Schwarzkopf Microanalytical Laboratory, Inc., Woodside, NY. Anal. Calcd for $C_{98}H_{112}N_8P_2Cl_2Ir_2$: C, 61.33; H, 5.88; N, 5.84; P, 3.23; Cl, 3.69. Found: C, 61.56; H, 5.92; N, 5.56; P, 2.89; Cl, 3.92.

Crystals suitable for X-ray diffraction were obtained by slow room-temperature evaporation of a mixed CH_2Cl_2–C_6H_6–*n*-C_6H_{14} solvent containing [(OEP)IrCl]$_2$dppe.

Crystal Structure Determination. Single-crystal X-ray analysis of [(OEP)IrCl]$_2$dppe was performed at the University of Houston X-ray Crystallographic Center. A small, dark cherry-colored block of approximate dimensions 0.20 × 0.22 × 0.44 mm was mounted on a glass fiber in a random orientation on a Nicolet R3m/V automatic diffractometer. Mo Kα radiation monochromatized by a highly ordered graphite crystal was used. Final cell constants as well as other information pertinent to data collection and refinement are listed in Table I. The Laue symmetry was determined to be $2/m$, and from the systematic absences noted, the space group was shown unambiguously to be $P2_1/c$. Intensities were measured by using the ω-scan technique, with the scan rate depending on the count obtained in rapid prescans of each reflection. Two standard reflections were monitored after every 2 h or every 100 data collected, and these showed linear decay amounting to 25% over the 5-day course of the experiment. A normalizing factor as a function of exposure time was applied to account for this. In the reduction of the data, Lorentz and polarization corrections were applied, as well as an empirical absorption correction based on ψ scans of ten reflections having χ values between 70 and 90°.

The structure was solved by use of the SHELXTL Patterson interpretation program, which revealed the position of the Ir atom in the asymmetric unit, consisting of half of the bridged diporphyrin molecule that lies about an inversion center. The remaining non-hydrogen atoms were located in subsequent difference Fourier syntheses. The usual sequence of isotropic and anisotropic refinements was followed, after which all hydrogens were entered in ideal calculated positions and constrained to riding motion, with a single nonvariable isotropic temperature factor. There is a 50:50 disorder of the C29–C30 ethyl group, and this was treated by refining isotropic rigid-body ethyls at each site. A molecule of benzene solvent was also located and refined to reasonable isotropic thermal parameters when the population was fixed at 75%. Initially, the benzene is probably present in full occupancy and the gradual loss accounts for the observed crystal decomposition. After all shift/esd ratios were less than 0.3, convergence was reached at the agreement factors listed in Table I. No unusually high correlations were noted between any of the variables in the last cycle of full-matrix least-squares refinement, and the final difference density map showed a maximum peak of about 1.2 e/Å^3, located quite close to Ir. All calculations were made by using Nicolet's SHELXTL PLUS (1987) series of crystallographic programs.

Table I. Data Collection and Processing Parameters

space group	$P2_1/c$, monoclinic	mol formula	$C_{98}H_{112}N_8P_2Cl_2Ir_2 \cdot 2C_6H_6$
fw	2075.66		
cell const		Z	2
a, Å	13.989 (4)	ρ(calc), g/cm^3	1.42
b, Å	19.864 (6)	μ, cm^{-1}	28.8
c, Å	17.752 (6)	λ(Mo Kα), Å	0.71073
β, deg	101.22 (2)	$R(F_o)$	0.045
V, Å^3	4839	$R_w(F_o)$	0.043

Results and Discussion

Synthesis. The reaction between (OEP)Ir(C_3H_7) and dppe in both benzene and CH_2Cl_2 was monitored by UV–visible spectroscopy. The reaction of this compound with PPh_3 is shown in Figure 1a and leads to (OEP)Ir(C_3H_7)(PPh_3), which has bands at 366, 424, and 530 nm in benzene. The reaction is rapid and is complete after the addition of 1.0 equiv of PPh_3, as shown by the inset in Figure 1a. The final spectrum of (OEP)Ir(C_3H_7)(PPh_3) has a split Soret band (see Table II) and is classified as a hyperspectrum.[15]

Spectral changes associated with the addition of dppe to benzene solutions of (OEP)Ir(C_3H_7) are shown in Figure 1b and are similar to those obtained upon complexation with PPh_3 (Figure 1a). The reaction is complete when 1.0 equiv of dppe is added to solution, and the final resulting spectrum is characterized by absorption bands at 367, 430, and 532 nm. A plot of the changes in absorbance at 390 and 430 nm as a function of [dppe] is depicted

(8) Guilard, R.; Kadish, K. M. *Comments Inorg. Chem.* **1988**, *7*, 287–305.
(9) Guilard, R.; Kadish, K. M. *Chem. Rev.* **1988**, *88*, 1121–1146.
(10) (a) Pringle, P. G.; Shaw, B. *J. Chem. Soc., Chem. Commun.* **1982**, *81*. (b) McEwan, D. M.; Pringle, P. G.; Shaw, B. *J. Chem. Soc., Chem. Commun.* **1982**, 859. (c) McDonald, W. S.; Pringle, P. G.; Shaw, B. *J. Chem. Soc., Chem. Commun.* **1982**, 861.
(11) Cotton, F. A.; Dunbar, K. R.; Eagle, C. T.; Falvello, L. R.; Price, A. C. *Inorg. Chem.* **1989**, *28*, 1754.
(12) Canich, J. A. M.; Cotton, F. A.; Daniels, L. M.; Lewis, D. B. *Inorg. Chem.* **1987**, *26*, 4046.
(13) Kadish, K. M.; Cornillon, J.-L.; Mitaine, P.; Deng, Y. J.; Korp, J. *Inorg. Chem.* **1989**, *28*, 2534.
(14) Lin, X-Q.; Kadish, K. M. *Anal. Chem.* **1985**, *57*, 1498.
(15) Gouterman, M. In *The Porphyrins*; Dolphin, D., Ed.; Academic Press: New York, 1978; Vol. III.

Table II. UV-Visible Spectroscopic Data for Selected Iridium(III) Octaethylporphyrins

compd	solvent	λ_{max}, nm ($10^{-3}\epsilon$)				
		Soret bands		Q bands		
$(OEP)Ir(C_3H_7)(PPh_3)$[a]	C_6H_6	366 (85)	424 (87)	530 (14.3)		
$(OEP)Ir(C_3H_7)(dppe)$		367 (59)	430 (52)	532 (10.4)		
$(OEP)Ir(Cl)(dppe)$	CH_2Cl_2	363 (78)	416 (124)	523 (20.9)	554 (24.0)	
$[(OEP)IrCl]_2dppe$			403 (204)	517 (22.0)	548 (39.7)	
$(OEP)Ir(CO)Cl$[b]			402 (170)	516 (11.4)	548 (28.1)	
$[[(OEP)IrCl]_2dppe]^{2+}$			394 (97.1)	518 (12.3)	548 (20.4)	603 (10.7)

[a] Reference 13. [b] Reference 17.

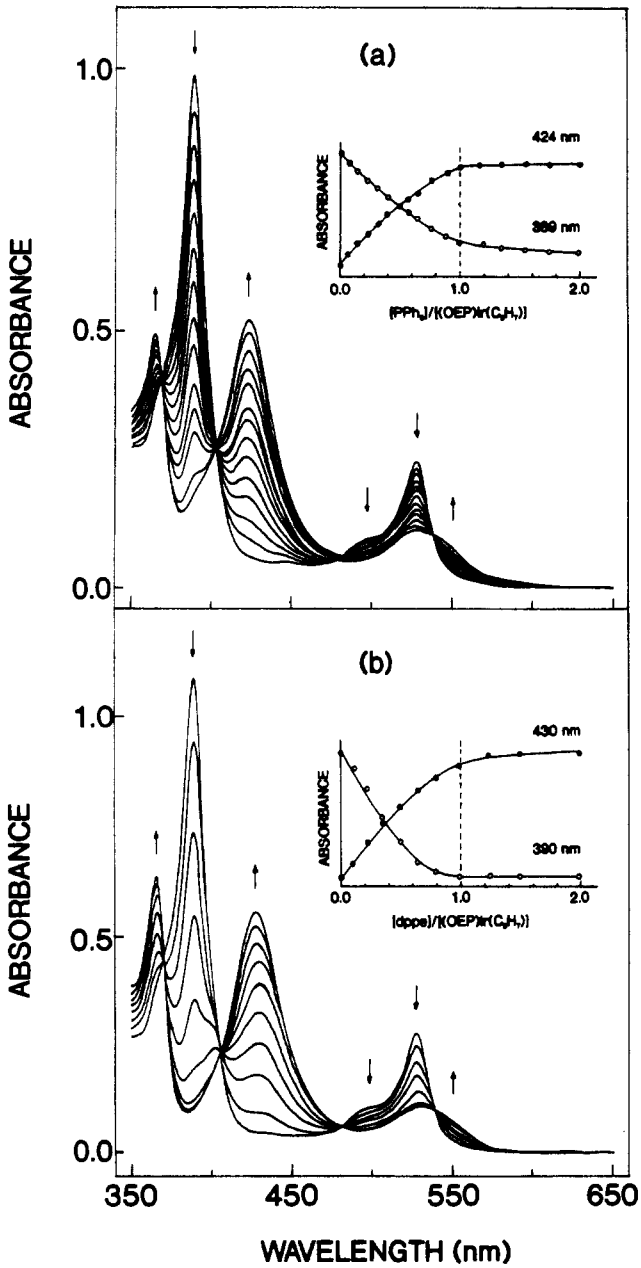

Figure 1. UV-visible spectral changes observed during a titration of $(OEP)Ir(C_3H_7)$ in benzene with (a) PPh_3 and (b) dppe.

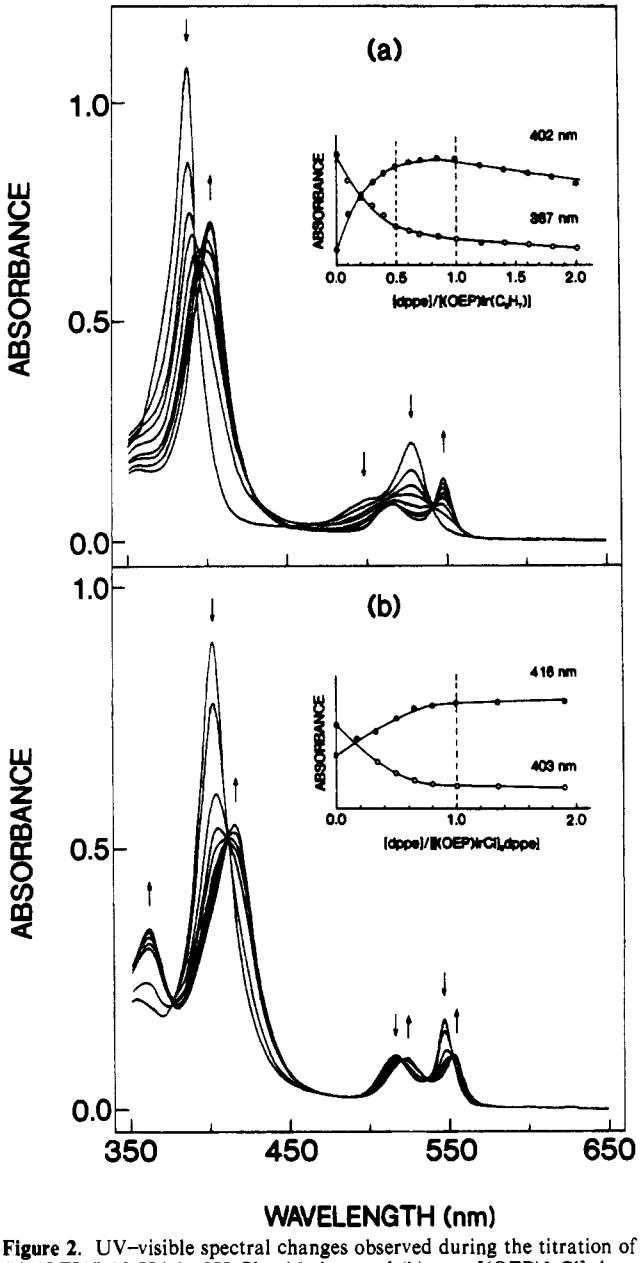

Figure 2. UV-visible spectral changes observed during the titration of (a) $(OEP)Ir(C_3H_7)$ in CH_2Cl_2 with dppe and (b) pure $[(OEP)IrCl]_2dppe$ in CH_2Cl_2 with dppe.

in the inset of Figure 1b, and an analysis of the data suggests the formation of monomeric six-coordinate $(OEP)Ir(C_3H_7)(dppe)$, as shown in eq 1.

$$(OEP)Ir(C_3H_7) + dppe \rightarrow (OEP)Ir(C_3H_7)(dppe) \quad (1)$$

The ligand addition reaction (1) does not occur in CH_2Cl_2, where completely different spectral changes are obtained (see Figure 2a). The titration of $(OEP)Ir(C_3H_7)$ with dppe in CH_2Cl_2 shows no isosbestic points and demonstrates that more than two spectroscopically detected species are present during the titration.

Also, the maximum change in the Soret band intensity is obtained when 0.5–0.6 equiv of dppe is added to solution. As will be shown, the final product formed in the reaction between $(OEP)Ir(C_3H_7)$ and dppe in CH_2Cl_2 is $[(OEP)IrCl]_2dppe$. A detailed mechanism for formation of the bimetallic complex has not been elucidated, but the overall reaction clearly involves Cl abstraction from CH_2Cl_2 to generate $[(OEP)IrCl]_2dppe$, as shown in eq 2.

$$2(OEP)Ir(C_3H_7) + dppe \xrightarrow{CH_2Cl_2} [(OEP)IrCl]_2dppe + \text{byproducts} \quad (2)$$

Table III. Atomic Coordinates (×10^4) and Their Estimated Standard Deviations

	x	y	z
Ir	1144 (1)	1236 (1)	1801 (1)
Cl	1141 (3)	2165 (3)	2681 (3)
P	1133 (3)	338 (3)	1011 (3)
N1	40 (10)	801 (7)	2249 (8)
N2	123 (10)	1748 (7)	1017 (8)
N3	2237 (9)	1709 (7)	1404 (8)
N4	2152 (12)	787 (7)	2624 (8)
C1	161 (17)	362 (10)	2876 (11)
C2	-833 (15)	184 (10)	2990 (12)
C3	-1477 (15)	533 (11)	2458 (13)
C4	-933 (15)	904 (9)	1978 (10)
C5	-1331 (12)	1301 (10)	1362 (11)
C6	-872 (15)	1698 (10)	934 (11)
C7	-1290 (15)	2109 (10)	282 (12)
C8	-601 (18)	2424 (11)	-4 (14)
C9	371 (19)	2197 (10)	480 (13)
C10	1235 (15)	2391 (10)	384 (12)
C11	2111 (14)	2175 (10)	825 (11)
C12	3132 (58)	2320 (15)	689 (24)
C12′	3059 (58)	2428 (20)	771 (19)
C13	3704 (14)	2026 (10)	1234 (12)
C14	3240 (15)	1599 (9)	1652 (12)
C15	3617 (13)	1202 (10)	2242 (10)
C16	3162 (14)	822 (9)	2715 (11)
C17	3558 (14)	421 (10)	3375 (11)
C18	2837 (17)	119 (10)	3641 (11)
C19	1944 (15)	374 (10)	3174 (12)
C20	1065 (15)	175 (9)	3296 (9)
C21	-1000 (15)	-311 (10)	3603 (11)
C22	-947 (16)	-1015 (10)	3356 (12)
C23	-2544 (14)	542 (11)	2389 (10)
C24	-2887 (13)	1138 (12)	2787 (11)
C25	-2397 (15)	2158 (11)	-47 (13)
C26	-2787 (17)	2680 (13)	373 (15)
C27	-680 (17)	2878 (11)	-711 (14)
C28	-564 (18)	3545 (12)	-413 (13)
C29	3191	2722	-28
C29′	3218	3022	272
C30	2971	3475	82
C30′	3019	2821	-587
C31	4813 (16)	2084 (12)	1384 (14)
C32	5166 (14)	1541 (13)	931 (12)
C33	4657 (15)	376 (11)	3633 (11)
C34	5063 (16)	991 (14)	4117 (13)
C35	2918 (17)	-371 (13)	4289 (11)
C36	2728 (20)	-86 (16)	4980 (15)
C37	2039 (14)	331 (12)	421 (11)
C38	2763 (20)	-138 (13)	464 (12)
C39	3429 (19)	-93 (17)	-37 (20)
C40	3345 (26)	455 (22)	-554 (16)
C41	2587 (24)	872 (16)	-581 (19)
C42	1988 (17)	835 (13)	-104 (13)
C43	1185 (16)	-464 (8)	1516 (9)
C44	377 (17)	-847 (12)	1514 (11)
C45	437 (23)	-1435 (12)	1929 (14)
C46	1319 (27)	-1665 (12)	2340 (14)
C47	2091 (21)	-1289 (14)	2348 (13)
C48	2055 (18)	-700 (11)	1942 (11)
C49	23 (14)	294 (9)	307 (10)
C50	3504 (10)	3402 (10)	2460 (9)
C51	3852	2927	3025
C52	4798	2982	3453
C53	5395	3512	3315
C54	5046	3987	2749
C55	4101	3932	2321

A further reaction between dppe and [(OEP)IrCl]$_2$dppe can also occur and leads to monomeric (OEP)Ir(Cl)(dppe), as shown in eq 3.

$$[(OEP)IrCl]_2dppe + dppe \rightarrow 2(OEP)Ir(Cl)(dppe) \quad (3)$$

This latter reaction was demonstrated by a titration of pure [(OEP)IrCl]$_2$dppe with dppe in CH_2Cl_2 (see Figure 2b). The Soret band at 403 nm decreases in intensity upon the addition of dppe to solutions of [(OEP)IrCl]$_2$dppe in CH_2Cl_2, while new bands appear at 363 and 416 nm. Isosbestic points are located at 411, 484, 535, and 552 nm, and the reaction is complete after the addition of 1.0 equiv of dppe (see Figure 2b inset).

Table IV. Selected Bond Distances (Å)

Ir–Cl	2.417 (5)	Ir–N4	2.029 (14)
Ir–P	2.268 (5)	P–C37	1.794 (22)
Ir–N1	2.059 (15)	P–C43	1.823 (17)
Ir–N2	2.059 (13)	P–C49	1.796 (18)
Ir–N3	2.034 (14)	C49–C49′	1.59 (3)

Table V. Selected Bond Angles (deg)

Cl–Ir–P	177.8 (2)	N3–Ir–P	93.7 (4)
Cl–Ir–N1	88.6 (4)	N4–Ir–P	91.1 (4)
Cl–Ir–N2	88.4 (4)	Ir–P–C37	116.5 (8)
Cl–Ir–N3	88.1 (4)	Ir–P–C43	112.9 (6)
Cl–Ir–N4	87.7 (4)	Ir–P–C49	111.7 (6)
N1–Ir–N2	89.7 (6)	C37–P–C43	108.4 (11)
N1–Ir–N3	176.7 (5)	C37–P–C49	101.9 (9)
N1–Ir–N4	90.3 (6)	C43–P–C49	104.2 (9)
N1–Ir–P	89.6 (4)	P–C37–C38	124.9 (18)
N2–Ir–N3	90.4 (5)	P–C37–C42	116.4 (18)
N2–Ir–N4	176.0 (5)	P–C43–C44	122.2 (15)
N2–Ir–P	92.9 (4)	P–C43–C48	120.7 (16)
N3–Ir–N4	89.3 (6)	P–C49–C49′	115.3 (17)

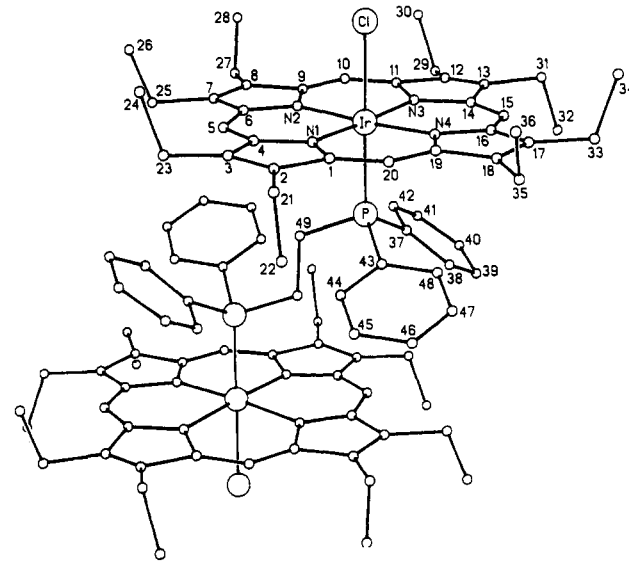

Figure 3. Molecular structure of [(OEP)IrCl]$_2$dppe, with hydrogens omitted for clarity.

Structural Characterization of [(OEP)IrCl]$_2$dppe. The bimetallic Ir(III) complex was isolated and crystallized as described in the Experimental Section. Final atomic positional parameters are listed in Table III, while Tables IV and V give selected bond distances and angles, respectively. [(OEP)IrCl]$_2$dppe contains two (OEP)Ir(Cl)(PPh$_2$) octahedra linked by $-CH_2CH_2-$ to yield a structure of C_i symmetry. The molecular structure and atom numbering scheme are shown in Figure 3. The crystal structure determination shows that the iridium has essentially octahedral coordination geometry, lying out of the N_4 plane by 0.065 Å and out of the mean porphyrin plane by 0.076 Å toward phosphorus. Similar results have been obtained for other iridium porphyrins.[13,16,17] The four Ir–N distances average 2.05 Å, in good agreement with values observed in a number of other iridium(III) octaethylporphyrins: 2.06 Å for (OEP)Ir(C_8H_{13}),[16] 2.05 Å for (OEP)Ir(CO)Cl,[17] 2.04 Å for (OEP)Ir(C_3H_7)(PPh$_3$),[13] and 2.03 Å for (OEP)Ir(C_3H_7)(Me$_2$SO).[13]

The axial Ir–P distance is 2.268 Å, similar to the Fe–P distance of 2.284 Å in (TPP)Fe(PMe$_2$Ph)$_2$[18] but significantly shorter than

(16) Cornillon, J.-L.; Anderson, J. E.; Swistak, C.; Kadish, K. M. *J. Am. Chem. Soc.* **1986**, *108*, 7633.
(17) Swistak, C.; Cornillon, J.-L.; Anderson, J. E.; Kadish, K. M. *Organometallics* **1987**, *6*, 2146.

the Ir–P distance of 2.537 Å found in the monomeric porphyrin $(OEP)Ir(C_3H_7)(PPh_3)$.[13] It is also much shorter than the Ir–PPh_3 bond lengths observed in non-porphyrin octahedral complexes: 2.43[19] and 2.38 Å.[20] However, it is comparable to the value of 2.32 Å found in an Ir–PMe_3 complex,[21] and it thus seems safe to conclude that the presence of one less phenyl group on P significantly reduces the steric interaction between the bridging ligand and the porphyrin macrocycle. The Ir–Cl distance (2.417 Å) is quite long compared to the value of 2.292 Å found in $(OEP)Ir(CO)Cl$[17] but falls within the range noted in several non-porphyrin octahedral complexes.[19-21] Some slight lengthening of the Ir–Cl bond in the present case may be due to the positioning of the metal out of the porphyrin plane toward phosphorus, conceivably resulting in minor electronic repulsion between the chlorine and the macrocycle ring.

The geometry of the dppe bridging ligand shows some unusual features. Although the average P–C distance of 1.80 Å is in good agreement with other metal phosphines,[18,22-24] as well as with triphenylphosphine oxide,[25] the angles about phosphorus show significant variation, with Ir–P–C ranging from 112 to 117° and C–P–C ranging from 102 to 108°. These values indicate significant differences in the environments of the phenyl rings, but the distortions are not nearly as great as those observed in some metal complexes having chelating dppe ligands.[23] The Ir–P–C43 angle is smaller than the Ir–P–C37 angle as a result of less torsional twist about the P–C43 bond; i.e., the C43 phenyl is closer to being coplanar with the porphyrin ring than is the C37 phenyl. This is evidenced by the larger difference in distances from the macrocycle plane for C38/C42 (0.98 Å) vs C44/C48 (0.42 Å). Both C43 and C49 are about the same distance from the macrocycle (3.01 Å), whereas the twist of its ring places C37 3.18 Å away. A similar but more exaggerated situation is observed in $(OEP)Ir(C_3H_7)(PPh_3)$, where the phenyl ring most nearly coplanar with the porphyrin has Ir–P–C = 108°, while the other two quite twisted rings have angles around 121°.[13] Obviously there is some steric interference involved, even with only two phenyl rings on the phosphorus. There also appears to be significant steric strain between the phenyls and the opposite porphyrin ring of the molecule, which can be seen in the unusually long ethylene distance (1.59 Å) and the larger than expected P–C49–C49′ angle (115°).

Electronic Absorption and ^1H NMR Spectroscopy. A number of different Ir(III) porphyrins have now been spectrally characterized.[13,16,17,26-30] These compounds can be divided into two groups, namely those with a single Soret band, which are classified as normal spectra, and those with a split Soret band, which are classified as hyperspectra.[15] The electronic absorption spectrum of $[(OEP)IrCl]_2$dppe in CH_2Cl_2 has bands at 403, 517, and 548 nm, all of which are similar to values for $(OEP)Ir(CO)Cl$[17,26] in CH_2Cl_2 (see Table II). Unlike other monomeric iridium[13] or iron porphyrin[31] alkylphosphine adducts, bimetallic $[(OEP)IrCl]_2$dppe does not exhibit a characteristic hyperporphyrin UV–visible spectrum. However, monomeric (OEP)Ir(Cl)(dppe) has a hyper character, as shown in Table II.

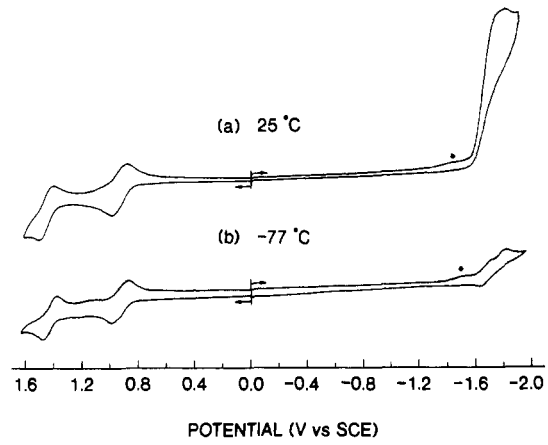

Figure 4. Cyclic voltammograms of 5.2×10^{-4} M $[(OEP)IrCl]_2$dppe in CH_2Cl_2, 0.1 M $(TBA)ClO_4$ (a) at 25 °C and (b) at −77 °C at a scan rate of 0.1 V/s. * peak is due to reduction of free (OEP)Ir(Cl)(dppe) (see text).

Table VI. Half-Wave Potentials (V vs SCE) for the Room-Temperature Oxidation and Reduction of Selected Iridium(III) Octaethylporphyrins

compd	solvent	oxidn		redn	
$[(OEP)IrCl]_2$dppe	CH_2Cl_2	1.44	0.93	−1.82[a]	
	PrCN	1.38	0.86	−1.66[a]	
(OEP)Ir(Cl)(dppe)	CH_2Cl_2		0.95[b]	−1.48	−1.75[a]
$(OEP)Ir(CO)Cl$[c]	CH_2Cl_2	1.45	1.05	−1.48[a]	

[a] E_{pc} at 0.1 V/s. [b] E_{pa} at 0.1 V/s. [c] Reference 17.

$[(OEP)IrCl]_2$dppe has ^1H NMR resonances at 9.06 (s, meso H), 3.74 (m, α-CH_2), and 1.56 ppm (t, β-CH_3) in $CDCl_3$. These values are generally consistent with NMR data reported in the literature for monomeric OEP complexes having a central metal in the +3 oxidation state.[32] The resonances of $[(OEP)IrCl]_2$dppe are also similar to those of $(OEP)IrCH_2CH(OEt)Ir(OEP)$,[33] which has two bridged (OEP)Ir units in an approximate trans position but are shifted upfield from those of some two dozen monomeric Ir(III) OEP complexes,[13,16,26,29] which have values of 9.56–10.52 (meso H), 3.86–4.20 (α-CH_2) and 1.78–1.98 ppm (β-CH_2).

The observed shifts of the ring proton signals in $[(OEP)IrCl]_2$dppe, especially those protons in the meso position, reflect a mutual influence of the diamagnetic ring currents produced by the two porphyrins. This is confirmed by the crystal structure, which shows that the edge of one porphyrin macrocycle is just above the center of the other macrocycle (see Figure 3).

Of some interest is the singlet resonance peak at $\delta = -5.74$ ppm, which is assigned to the ethylene group ($-CH_2CH_2-$) in the bridging ligand. This value is twice that observed for monomeric iron alkylphosphine porphyrin adducts:[18] i.e., −2.45 ppm for CH_3 in $(TPP)Fe(PMe_2Ph)_2$ and −2.93 ppm in $(TPP)Fe(PMe_3)(py)$, where py is pyridine. The phenyl groups of the bridging ligand have resonances at 2.72 (s, ortho H), 6.51 (t, meta H), and 7.2 ppm (m, para H), all of which are consistent with literature values.[18] It should be noted that the signal of the ortho protons in the phenyl groups is at much higher field than found in the axial phenyl groups of monomeric iron porphyrin $(TPP)Fe(PMe_2Ph)_2$[18] due to their close proximity to the porphyrin ring.

Electrochemistry. The oxidation and reduction of several σ-bonded and ionic Ir(III) porphyrins have been reported in the literature.[13,16,17,26] The electrochemical properties of these species are similar to each other in that they generally undergo reversible

(18) Sodano, P.; Simonneaux, G.; Toupet, L. *J. Chem. Soc., Dalton Trans.* **1988**, 2615.
(19) Clark, G. R.; Roper, W. R.; Wright, A. H. *J. Organomet. Chem.* **1982**, *236*, C7.
(20) Olgemöller, B.; Bauer, H.; Löbermann, H.; Nagel, U.; Beck, W. *Chem. Ber.* **1982**, *115*, 2271.
(21) Milstein, D.; Calabrese, J. C. *J. Am. Chem. Soc.* **1982**, *104*, 3773.
(22) Cogne, A.; Grand, A.; Laugier, J.; Robert, J. B.; Wiesenfeld, L. *J. Am. Chem. Soc.* **1980**, *102*, 2238.
(23) Kuchynka, D. J.; Kochi, J. K. *Organometallics* **1989**, *8*, 677.
(24) Ball, R. G.; Domazetis, G.; Dolphin, D.; James, B. R.; Trotter, J. *Inorg. Chem.* **1981**, *20*, 1556.
(25) Thierbach, D.; Huber, F.; Preut, H. *Acta Crystallogr., Sect. B* **1980**, *36*, 974.
(26) Sugimoto, H.; Ueda, N.; Mori, M. *J. Chem. Soc., Dalton Trans.* **1982**, 1611.
(27) Farnos, M. D.; Woods, B. A.; Wayland, B. B. *J. Am. Chem. Soc.* **1986**, *108*, 3659.
(28) Collman, J. P.; Kim, K. *J. Am. Chem. Soc.* **1986**, *108*, 7847.
(29) Ogoshi, H.; Setsune, J.; Yoshida, Z. *J. Organomet. Chem.* **1978**, *159*, 317.
(30) Kadish, K. M.; Deng, Y. J.; Yao, C.-L.; Anderson, J. E. *Organometallics* **1988**, *7*, 1979.
(31) Simonneaux, G.; Sodano, P. *Inorg. Chem.* **1988**, *27*, 3956.
(32) Janson, T. S.; Katz, J. J. In *The Porphyrins*; Dolphin, D., Ed.; Academic Press: New York, 1978; Vol. IV.
(33) Del Rossi, K. J.; Wayland, B. B. *J. Chem. Soc., Chem. Commun.* **1986**, 1653.

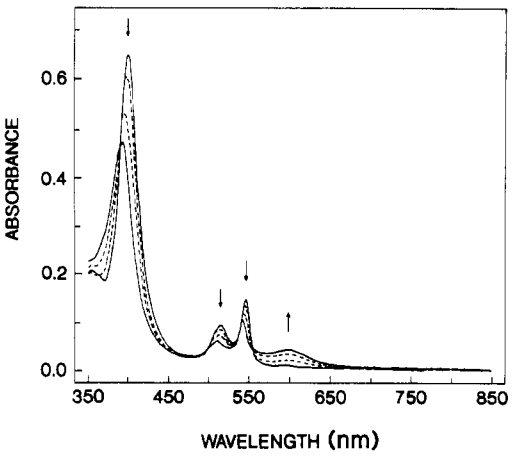

Figure 5. UV–visible spectral changes observed during the first oxidation of [(OEP)IrCl]$_2$ dppe in PrCN, 0.2 M (TBA)ClO$_4$.

oxidations and irreversible reductions. However, they do seem to vary with respect to the site of electron transfer. For example, (OEP)Ir(C_8H_{13}) undergoes a one-electron oxidation at the σ-bonded C_8H_{13} ligand,[16] while the one-electron oxidation of (OEP)Ir(CO)Cl occurs at the porphyrin π ring system.[17] Both compounds undergo a reversible one-electron reduction by cyclic voltammetry at low temperature or fast potential scan rates, but at room temperature an irreversible two-electron reduction occurs, and the final spectral product on the bulk electrolysis time scale is assigned as [(OEP)Ir]$^-$ in both cases.

[(OEP)IrCl]$_2$dppe undergoes a similar type of electrochemical reactivity as shown in Figure 4a. There are two reversible room-temperature oxidations in either CH_2Cl_2 or PrCN. The first occurs at an $E_{1/2}$ between 0.86 and 0.93 V, while the second is located between 1.38 and 1.44 V vs SCE (see Figure 4 and Table VI). Both oxidations are diffusion controlled, as evidenced by a constant value of $i_p/v^{1/2}$ and an invariance of the anodic and cathodic peak potentials with increase in scan rate. Bulk controlled-potential coulometry at +1.10 V in CH_2Cl_2 or at +1.00 V in PrCN gives a coulometric value of $n = 2.0 \pm 0.1$, indicating an overall two-electron abstraction in the first oxidation of [(OEP)IrCl]$_2$dppe.

The measured $|E_{pa} - E_{pc}|$ for the first oxidation of [(OEP)IrCl]$_2$dppe is 100 mV in CH_2Cl_2 and 80 mV in PrCN, both of which are higher than the theoretical 60 mV expected for a multiple-electron-transfer process for a molecule containing two or more noninteracting redox centers.[34] This peak-to-peak separation does not change over a scan rate range of 0.05–0.5 V/s and indicates that there are two closely separated $E_{1/2}$ values for the first oxidation of [(OEP)IrCl]$_2$dppe.

The UV–visible spectrum of the species formed during controlled-potential oxidation of [(OEP)IrCl]$_2$ dppe at +1.00 V in PrCN, 0.2 M (TBA)ClO$_4$ is shown in Figure 5 and resembles that of a porphyrin π cation radical.[35] Similar spectral changes are also observed during controlled-potential oxidation of the complex in CH_2Cl_2, and the final spectrum in CH_2Cl_2 is also typical of a porphyrin π cation radical. The assignment of such a radical after the two-electron oxidation at $E_{1/2} = 0.93$ V in CH_2Cl_2 was confirmed by ESR spectroscopy. The oxidized species does not exhibit a room-temperature ESR signal in CH_2Cl_2, but at −77 °C a well-defined signal is located at $g = 2.001 \pm 0.002$ with $\Delta H_{pp} = 24$ G. The fact that two electrons are coulometrically abstracted in the first oxidation step thus suggests that one electron is abstracted from each OEP ring to form a porphyrin biradical.[36] The larger than expected separation in $|E_{pa} - E_{pc}|$ is attributed to separate but closely spaced one-electron oxidations. The fact that

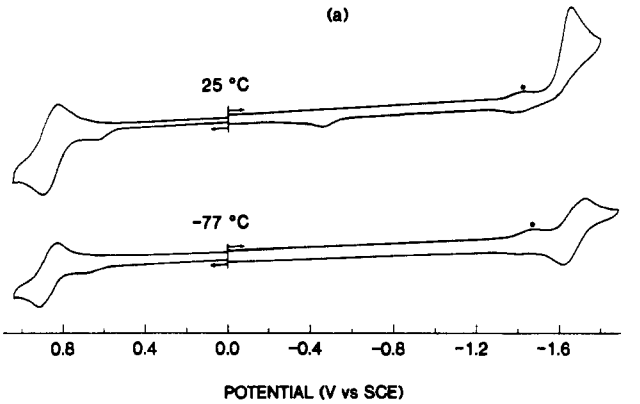

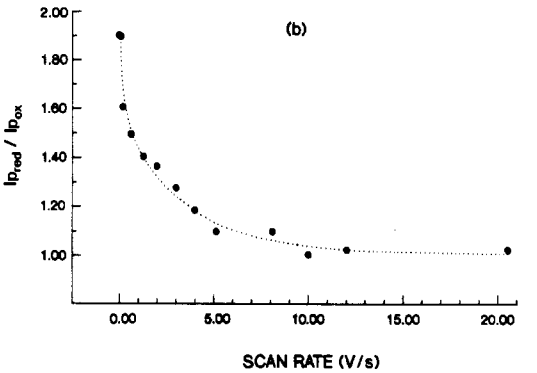

Figure 6. (a) Cyclic voltammograms of 5.2×10^{-4} M [(OEP)IrCl]$_2$dppe in PrCN, 0.2 M (TBA)ClO$_4$ at 25 °C and at −77 °C at a scan rate of 0.1 V/s. (b) Ratio of peak currents for the first reduction and the first oxidation of [(OEP)IrCl]$_2$dppe as a function of scan rate at 25 °C in PrCN. * peak is due to reduction of free (OEP)Ir(Cl)(dppe) (see text).

the $E_{1/2}$ values for oxidation of the two porphyrin rings are not identical indicates that the single unpaired electrons in each porphyrin fragment are coupled with each other to some extent at room temperature even though they are connected by a nonconjugated bridging ligand.

A decrease in temperature from −77 to −140 °C results in stronger ESR signals with smaller peak-to-peak separations. This suggests that the interaction between these two unpaired electrons decreases at lower temperatures. At −140 °C, there is a signal at $g = 2.001$ with a doublet hyperfine splitting of 10.8 G, which most probably arises from a coupling of the unpaired electron to the phosphorus nucleus ($I = {}^1/_2$). Thus, the unpaired electrons might be localized around the iridium atom at this lower temperature. Electrooxidized [(OEP)IrCl]$_2$dppe does not show an ESR signal in PrCN at temperatures between +25 and −110 °C, but at −150 °C a strong ESR signal at $g = 2.001$ with $\Delta H_{pp} = 9$ G is observed. There is, however, no hyperfine splitting of the signal in this solvent.

[(OEP)IrCl]$_2$dppe undergoes one irreversible room-temperature reduction by conventional voltammetry in CH_2Cl_2, 0.1 M (TBA)ClO$_4$. The current for this reduction in CH_2Cl_2 is much larger than that for the first oxidation of the compound under the same experimental conditions (see Figure 4a) and seems to involve a catalytic reaction of the reduced product with the CH_2Cl_2 solvent. Similar types of EC catalytic reductions have been observed for electrogenerated [(P)Co^I]$^-$[37] and [(P)Ni^I]$^-$[38,39] in CH_2Cl_2. The current for reduction of [(OEP)IrCl]$_2$dppe is much decreased in magnitude at −77 °C, as shown in Figure 4b. Under these conditions, the voltammogram is characterized by peaks at

(34) Flanagan, J. B.; Margel, S.; Bard, A. J.; Anson, F. C. *J. Am. Chem. Soc.* **1978**, *100*, 4248.
(35) Kadish, K. M. *Prog. Inorg. Chem.* **1986**, *34*, 435.
(36) Wertz, J. E.; Bolton, J. R. *Electron Spin Resonance—Elementary Theory and Practical Applications*; Chapman and Hill: New York, 1986; p 250.
(37) (a) Kadish, K. M.; Lin, X. Q.; Han, B. C. *Inorg. Chem.* **1987**, *26*, 4161. (b) Maiya, G. B.; Han, B. C.; Kadish, K. M. *Langmuir* **1989**, *5*, 645.
(38) Kadish, K. M.; Sazou, D.; Liu, Y. M.; Maiya, G. B.; Han, B. C.; Saoiabi, A.; Ferhat, M.; Guilard, R. *Inorg. Chem.* **1989**, *28*, 2542.
(39) Stolzenberg, A. M.; Stershic, M. T. *J. Am. Chem. Soc.* **1988**, *110*, 6391.

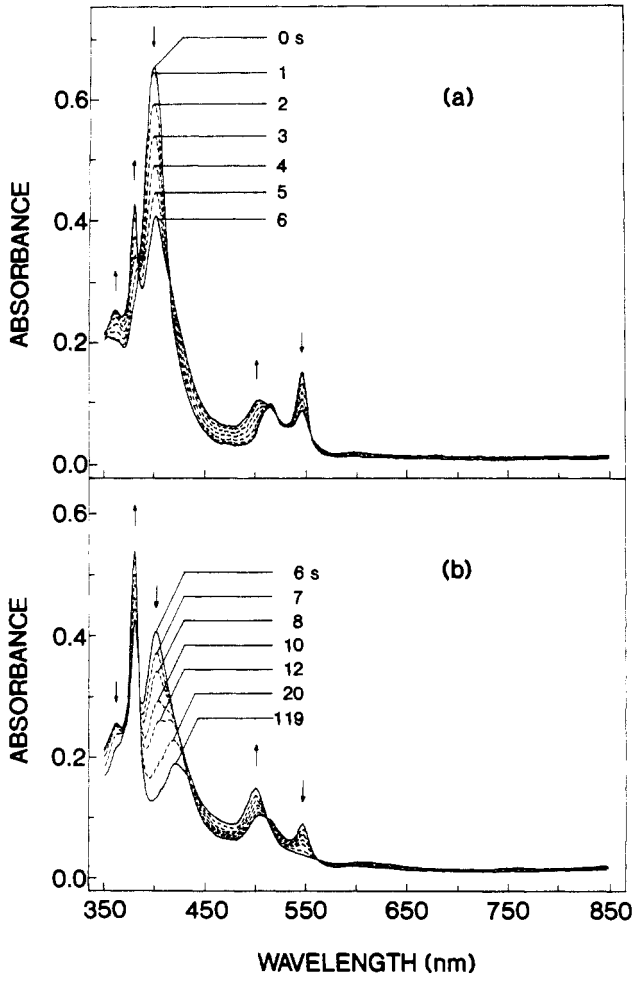

Figure 7. UV–visible spectral changes observed during the first reduction of $[(OEP)IrCl]_2dppe$ in PrCN, 0.2 M $(TBA)ClO_4$ (a) from 0 to 6 s and (b) from 6 to 119 s.

$E_{1/2} = -1.45$ V, $E_{1/2} = -1.67$ V, and $E_p = -1.82$ V. The first reversible peak is also present in solutions of $[(OEP)IrCl)]_2dppe$ containing 1–2 equiv of dppe and is assigned as a reaction of (OEP)Ir(Cl)(dppe), which appears to form upon dissociation of $[(OEP)Ir(Cl)]_2dppe$ prior to electroreduction. The latter two processes are associated with $[(OEP)IrCl]_2dppe$ but were not further analyzed in CH_2Cl_2 solvent, which is quite reactive.

The reduction of $[(OEP)IrCl]_2dppe$ is better defined in PrCN, as shown in Figure 6a. The ratios of currents for the first reduction (−1.66 V) to the first oxidation (0.86 V) of $[(OEP)IrCl]_2dppe$ are plotted in Figure 6b as a function of the scan rate at room temperature in PrCN. As can be seen, an increase in scan rate results in a current ratio which decreases from ~1.9 to ~1.0, clearly indicating an ECE-type mechanism on the reduction. A similar plot was obtained and a similar ECE mechanism proposed for the stepwise two-electron reduction of (OEP)Ir(CO)Cl in CH_2Cl_2.[17] These results for $[(OEP)IrCl]_2dppe$ were also confirmed by a low-temperature voltammogram, Figure 6a. At −77 °C, the peak current for reduction at $E_{1/2} = -1.67$ V is about equal to the peak current for oxidation at $E_{1/2} = 0.87$ V.

The voltammetric data in Figure 6 suggest that two different species might be spectroscopically detected during the electroreduction of $[(OEP)IrCl]_2dppe$. This is indeed the case, as shown by thin-layer UV–visible spectra obtained during controlled-potential reduction of $[(OEP)IrCl]_2dppe$ at −1.80 V in PrCN, 0.2 M $(TBA)ClO_4$, depicted in Figure 7. Figure 7a shows the spectral changes obtained during the first 6 s of electrolysis, while Figure 7b shows the spectra at times between 6 and 119 s. As the reduction of $[(OEP)IrCl]_2dppe$ initially proceeds, the original bands at 402 and 548 nm decrease in intensity, while the band at 517 nm shifts to 502 nm (see Figure 7a). At the same time, new peaks for the product appear at 363 and 381 nm. Isosbestic points are located at 385, 417, 514, and 555 nm, thus suggesting that only one spectrally detected species is generated at this stage of the reduction. However, after 2 min of controlled-potential reduction, the peaks at 363 and 548 nm have decreased in intensity and finally disappeared. New isosbestic points are located at 385, 513, and 561 nm, and the final product has bands at 381, 422, and 502 nm. This spectrum is similar to the one reported for $[(OEP)Ir]^-$ (382 and 502 nm) upon reduction of (OEP)Ir(CO)Cl in PhCN.[17]

The thin-layer cyclic voltammogram of $[(OEP)IrCl]_2dppe$ shows a ratio of reduction to oxidation peak currents that is about equal to 2.0. Thus, the cyclic voltammetric and spectral data are consistent with an overall four-electron reduction of $[(OEP)IrCl]_2dppe$ to give $[(OEP)Ir]^-$ as a final product on the thin-layer voltammetric time scale. A similar spectral product has been proposed for monomeric (OEP)Ir(CO)Cl, which undergoes an overall two-electron reduction via an ECE mechanism to generate $[(OEP)Ir]^-$ as a final product.[17]

No ESR signal was observed after bulk electroreduction of $[(OEP)IrCl]_2dppe$ either at room temperature or at −140 to −150 °C in CH_2Cl_2 or PrCN. This is consistent with the ultimate generation of $[(OEP)Ir]^-$. However, it should also be noted that the bulk controlled-potential reduction of $[(OEP)IrCl]_2dppe$ in PrCN resulted in a formation of metallic iridium, which deposited as brownish metal on the surface of the stirring bar. Electrochemically initiated demetalation of nickel[40] and silver[41] porphyrins has been reported in the literature, but this is the first example of demetalation for a reduced iridium porphyrin.

Electrochemistry of (OEP)Ir(Cl)(dppe). A titration of $[(OEP)IrCl]_2dppe$ with dppe was electrochemically monitored in CH_2Cl_2. When excess dppe is added to $[(OEP)IrCl]_2dppe$ in CH_2Cl_2, the first oxidation becomes irreversible and the reduction potential shifts anodically. The bridging dppe ligand is electrochemically inactive over a potential range of +1.10 to −2.0 V in CH_2Cl_2. On the basis of the spectroscopic data, the final product of the titration is assigned as (OEP)Ir(Cl)(dppe), which undergoes an irreversible oxidation at $E_p = 0.95$ V, a reversible reduction at $E_{1/2} = -1.48$ V, and an irreversible reduction at $E_p = -1.75$ V for a scan rate of 0.1 V/s at room temperature. These potentials differ from those of other iridium(III) porphyrins such as $(OEP)Ir(C_3H_7)(PPh_3)$[13] and $(OEP)Ir(C_3H_7)(P(OEt)_3)$,[13] which are more difficult to reduce. This difference in reduction potentials can be attributed to the electron-withdrawing Cl on (OEP)Ir(Cl)(dppe), which makes it easier to reduce but more difficult to oxidize, by lowering the electron density on either the metal or the whole complex. The much more positive reduction peak of (OEP)Ir(Cl)(dppe) compared to $[(OEP)IrCl]_2dppe$ may also explain the hyper character of its UV–visible spectrum.[15]

Summary. The electrochemical and spectroscopic data for neutral and electrooxidized $[(OEP)IrCl]_2dppe$ indicate that a weak electronic interaction exists between the two porphyrin macrocycles. Unlike iron porphyrins having single-atom bridging ligands,[1-5] the two porphyrin units in $[(OEP)IrCl]_2dppe$ have interactions that may be mediated through space rather than through bonding.[42]

Acknowledgment. The support of the National Science Foundation (Grant CHE-8515411) is gratefully acknowledged.

Supplementary Material Available: Tables of hydrogen atomic coordinates, anisotropic thermal parameters, and all intramolecular distances and angles (4 pages); a listing of observed and calculated structure factors (17 pages). Ordering information is given on any current masthead page.

(40) Kadish, K. M.; Sazou, D.; Liu, Y. M.; Saoiabi, A.; Ferhat, M.; Guilard, R. *Inorg. Chem.* **1988**, *27*, 1198.
(41) Kadish, K. M.; Lin, X. Q.; Ding, J. Q.; Wu, Y. T.; Araullo, C. *Inorg. Chem.* **1986**, *25*, 3236.
(42) Richardson, D. E.; Taube, H. *Coord. Chem. Rev.* **1984**, *60*, 607.